FEBS Letters

FEBS PRESS science publishing by scientists

Novel immunoassays to detect methionine adenosyltransferase activity and quantify *S*-adenosylmethionine

Xiujuan Hao[1], Min Zhou[2], Huijun Li[2] and Isaac A. Angres[1]

1 Arthus Biosystems, Richmond, CA, USA
2 Hunan SkyWorld Biotechnologies Co. Ltd., Hunan, China

Correspondence
X. Hao, Arthus Biosystems, 2600 Hilltop Dr., Richmond, CA 94806, USA
Fax: +1 844 448 7410
Tel: +1 844 486 3175
E-mail: sheryl.hao@arthusbio.com

(Received 4 February 2017, revised 12 March 2017, accepted 16 March 2017)

doi:10.1002/1873-3468.12631

Edited by Stuart Ferguson

We present a novel real-time immunoassay to measure methionine adenosyltransferase (MAT) activity that integrates the MAT-catalyzed reaction of Met and adenosine triphosphate to produce *S*-adenosylmethionine (SAM) and a highly sensitive immunoassay to specifically quantify SAM simultaneously. The cellular localization of SAM and *S*-adenosylhomocysteine varies with cell proliferation status: in normal cells, they are found mostly in the cytoplasm, but localize to the nucleus in proliferating cells. MAT-I/III activity is stimulated by Met, but inhibited by *S*-nitrosoglutathione, and the methylation index (MI) increases after Met stimulation of L02 cells. Met and *S*-nitrosoglutathione inhibit MAT-II activity, and the MI decreases after Met stimulation of HepG2 cells. The method described provides a significant advancement in the field for the measurement of MAT activity under various conditions.

Keywords: carcinogenesis; hepatocellular carcinoma; immunoassay; methionine adenosyltransferase; methylation index; *S*-adenosylmethionine

S-adenosylmethionine (SAM) is the key molecule of the methionine cycle and is critical to the basic metabolic pathways of all organisms. Most dietary methionine is converted to SAM in the liver, where up to 85% of all methylation reactions occur [1,2]. The first step of methionine metabolism is catalyzed by methionine adenosyltransferase (MAT, EC 2.5.1.6) [3]. The cells of nearly all organisms contain MAT, and MAT genes have been exceptionally conserved throughout evolution. In mammals, three isozymes of MAT encoded by three MAT genes have been identified. The *MAT1α* gene encodes the α1 catalytic subunit. MAT-I is a tetramer of α1, and MAT-III is a dimer of α1 subunits. Both MAT-I and MAT-III are present in the adult liver. MAT-II is a heterotetramer formed by the α2 catalytic subunit, which is encoded by the *MAT2α* gene, and the β subunit, which is encoded by *MAT2β*. MAT-II is present in nonliver cells, the embryonic liver, and hepatoma cells [4]. MAT-III is responsible for clearing Met after a high-Met meal. MAT-I/III maintains basal SAM levels required by the liver under fasting conditions [5].

The reactions catalyzed by MAT include (a) the catalysis of the reaction between Met and adenosine triphosphate (ATP) to generate SAM and tripolyphosphate (PPPi) and (b) the decomposition of PPPi to dimeric phosphoric acid (PPi) and inorganic monophosphate (Pi) *via* the phosphatase activity of

Abbreviations
ATP, adenosine triphosphate; CTCF, CCCTC-binding factor; DAPI, 4′,6-diamidino-2-phenylindole; FBS, fetal bovine serum; FCM, flow cytometry; GSNO, *S*-nitrosoglutathione; HBSS, Hank's Balanced Salt Solution; HCC, hepatocellular carcinoma; HRP, horseradish peroxidase; MAT, methionine adenosyltransferase; MEM, minimum essential medium; MI, methylation index; MTA, methylthioadenosine; Pi, inorganic monophosphate; PPi, dimeric phosphoric acid; PPPi, tripolyphosphate; SAH, *S*-adenosylhomocysteine; SAM, *S*-adenosylmethionine.

MAT. SAM has extremely diverse, important biological functions in nature. As the sole methyl donor in the vital methylation processes in humans, SAM plays critical roles in transmethylation, transsulfuration, and aminopropylation reactions. These functions imply that SAM and MAT are directly involved in methylation-related cellular regulation and function, methylthioadenosine (MTA)-regulated anti-inflammatory processes, polyamine synthesis, and the regulation of the ratio of Met to homocysteine. Therefore, both SAM and MAT have significant impacts on many processes that are essential to life, including metabolism, cell proliferation, differentiation, and apoptosis [6].

The methods for measuring MAT activity include (a) HPLC and LC-MS/MS to assess SAM [4,7] synthesis and (b) malachite green and ammonium molybdate to determine the content of Pi [8]. Method (a) has the following limitations: (i) the synthesized SAM cannot be measured immediately right after synthesis due to the length of time required for sample preparation and measurement, considering the highly instable nature of SAM, the accuracy of this method is reduced; (ii) newly synthesized SAM associated with MAT is not released immediately, and thus, chromatographic technologies cannot detect the unreleased SAM. Method (b) has the following limitations: (i) malachite green can bind to Pi, PPPi, and PPi, leading to inaccurate results; (ii) the sensitivity is low; (iii) the indirect method is subject to high variability; (iv) the triphosphatase activity of MAT is greatly influenced by the substrate Met, and thus, the reliability is poor; and (v) the phosphatase and SAM synthesis activities of MAT are likely not correlated and can be regulated differently, and thus, it may not be appropriate to use the phosphatase activity as an indicator of the SAM synthetic ability of MAT. Due to their critical limitations, these methods cannot sensitively and accurately reflect subtle changes in MAT activity. Therefore, a fast, convenient, accurate, sensitive, and specific method to measure MAT activity is urgently needed to overcome the limitations of the existing methods.

We established a highly sensitive real-time immunoassay of MAT activity to investigate how MAT activity is regulated in cells, particularly liver cells, and to explore the roles of SAM and the methylation index (MI) in liver cell proliferation and/or malignant transformation. 'Real-time' in here means the product of MAT-catalyzed biochemical reaction SAM is measured immediately with an immunoassay without any delay to reflect MAT activity instead of having to isolate molecularly unstable SAM and then measure it with much delay. A more accurate and sensitive method of measuring MAT activity is essential for elucidating the regulation of MAT genes and any changes in SAM reserves, particularly in the liver, which is the key organ in the Met cycle and SAM metabolism. The developed immunoassay of MAT activity was performed in two types of liver cell lines that express different MAT genes to examine some of the important processes of the Met cycle in normal and cancerous hepatocytes. In the present study, we used immunofluorescence, ELISA and flow cytometry (FCM) to examine SAM and *S*-adenosylhomocysteine (SAH) in cell lines and mouse primary liver cells to further investigate MAT activity and changes in SAM and the MI during carcinogenesis.

Experimental procedures

Materials

Met, SAH, Adenosine, MTA, ADP, ATP, *S*-nitrosoglutathione (GSNO), and trypsin were purchased from Sigma-Aldrich (St. Louis, MO, USA). MAT from ABXBIO (Beijing, China). Fetal bovine serum (FBS), culture media, and 4′,6-diamidino-2-phenylindole (DAPI) were obtained from Thermo-fisher Scientific (Waltham, MA, USA). All SAM and SAH reagents were from Arthus Biosystems (Richmond, CA, USA). FITC-labeled goat anti-(mouse IgG) was purchased from Abcam (Cambridge, UK). FCM fixation/permeabilization buffers were obtained from eBioscience (San Diego, CA, USA).

Immunofluorescent cell smears

L02 and HepG2 cells were inoculated on sterilized glass slides and were washed once with sterilized PBS. Minimum essential medium (MEM) containing 0.5 mM Met was added and the cells were cultured for 24 h. The slides were fixed with ice-cold acetone and were blocked with 0.5% skim milk. Next, 100 μL of 8 $\mu g \cdot mL^{-1}$ Alexa Fluor® 647-anti-SAM antibody and 40 $\mu g \cdot mL^{-1}$ Alexa Fluor® 488-anti-SAH antibody were added. The slides were then incubated for 45 min in the dark and washed. To counterstain the nuclei, the slides were incubated with 100 μL of DAPI for 20 min. The glass slides were sealed and photographed using laser scanning confocal microscopy (LSCM) Zeiss LSM 780 (Carl Zeiss Microscopy Ltd, Cambridge, UK).

MAT activity assay

Methionine adenosyltransferase samples, ATP and Met were prepared in buffer (150 mM KCl, 20 mM $MgSO_4$, and 100 mM Tris pH 7.42), and horseradish peroxidase (HRP)-conjugated anti-SAM antibody was added to a microtiter plate coated with SAM antigen. The plate was incubated at 37°C for 60 min, washed and then TMB substrate was

added for 15 min. The OD_{450} was determined using a Multiskan™, FC Microplate Photometer (Thermo Fisher Scientific, Waltham, MA, USA). One unit of enzyme activity was defined as the amount of MAT required to produce 1 nM SAM at 37°C per minute. The averages and standard deviations were calculated from three experiments, and statistical analysis was performed to identify significant differences between groups.

MAT activity in L02 and HepG2 cells in response to GSNO and Met

Cells were incubated with serum-free MEM containing 1 mM for 30 min. Different amounts of Met (0, 0.5, 1 and 2 mM) were added to the MEM containing 5% FBS and 2 mM glutamine and the cells were cultured for 24 h. The SAM levels were quantified immediately as follows: 1 mL of cell suspension from the above procedure was sonicated in an ice bath for 5 min, 10 μL supernatant was used to measure SAM using an ELISA kit, and the number of cells before homogenization was 2×10^7 for all groups.

FCM procedure

Cell suspension was prepared in PBS at 10^6 cells per sample and 100 μL of fixation buffer was added. The samples were incubated in dark at room temperature for 30 min. The cells were washed with 100 μL of permeabilization buffer and then incubated with 100 μL permeabilization buffer for 20 min. The samples were resuspended in 100 μL permeabilization buffer, and 10 μL of fluorescently labeled antibodies was added. The final concentrations of the Alexa Fluor® 647-anti-SAM antibody and the Alexa Fluor® 488-anti-SAH antibodies were approximately 4.5 and 45 $\mu g \cdot mL^{-1}$, respectively. The cells were incubated for 30 min, washed twice with PBS and resuspended in 0.5 mL of PBS for measurement using a BD FACSCanto II Flow Cytometer (BD, Franklin Lakes, NJ, USA).

Isolation and culture of mouse primary liver cells

The mice were first anesthetized with isoflurane. An incision was then made in the lower abdomen and extended vertically until the liver, portal vein, and inferior vena cava were exposed. The liver was perfused with Hank's Balanced Salt Solution (HBSS) at 7–9 $mL \cdot min^{-1}$ for 8 min to drain the blood, and then the HBSS was replaced with digestion medium until the liver began to swell. The swollen liver was excised and placed in a 10-cm dish containing digestion medium. The homogenate was triturated three times and filtered through a 70–75 μm membrane. The samples were spun at 50 ***g*** at 4°C for 2 min in a swinging-arm centrifuge, and the supernatant was aspirated using a sterile glass Pasteur pipette and cold isolation medium. The previous steps were then repeated twice. The cells were stained with trypan blue to confirm cell viability and inoculated into flasks.

Measurement of SAM and SAH in hepatic cell lines and mouse primary liver cells using FCM

Prior to Met stimulation, L02 and HepG2 cells were inoculated into 75 cm^2 culture flasks and cultured with RPMI 1640 containing 10% FBS. The medium was removed when the cells reached approximately 70% confluence. Minimum essential medium (MEM) containing 0.5 and 1 mM Met was added to L02 and HepG2 cells, respectively, and the cells were cultured for 24 h. Intracellular and nuclear SAM and SAH levels were measured using FCM. Mouse primary liver cells were inoculated into 75-cm^2 culture flasks and immediately cultured in Dulbecco's modified Eagle's medium for 20 h. Met-deprived MEM and MEM containing 0.5 or 1 mM Met were then added, and the cells were cultured for another 24 h before measuring SAM and SAH with FCM.

Measurement of cell cycle phases

L02, HepG2, K562, and MCF cells (2×10^6) were collected and washed with PBS, and 3 mL of cold anhydrous ethanol was added dropwise to 1 mL of cell suspension. The samples were immediately mixed and incubated on ice for 30 min. The cell suspension was washed and 400 μL of sodium citrate solution (38 mM), 15 μg of propidium iodide, and 10 μg of RNase were added. The samples were incubated at 37°C in the dark for 30 min, followed by cell analysis using a BD FACSCanto II Flow Cytometer to determine the DNA content.

Statistical analysis

GRAPHPAD PRISM 4.0 (GraphPad Prism Inc., San Diego, CA, USA) was used for ANOVA analysis of the ELISA and FCM results. Significance was determined at $P \leq 0.05$.

Results

A novel method for the assessment of MAT activity

The anti-SAM antibody must have high specificity for use in an immunoassay to monitor the SAM synthesis because the substrates ATP and Met and the product SAM are present in the same system. Any cross-reaction of Met or ATP with the anti-SAM antibody interferes with the competition and affects the binding of the SAM product to the HRP-conjugated anti-SAM antibody. The results on antibody specificity and MAT-catalyzed SAM synthesis can be found in our previously

published work (http://bmcresnotes.biomedcentral.com/articles/10.1186/s13104-016-2296-8). The measurement of SAM by competitive ELISA was very sensitive to small changes in MAT activity, and the SAM synthesized by MAT was linearly related to the reaction time during the first 60 min of the reaction. After 60 min, a reaction plateau was reached under the test conditions. To increase MAT activity and the detection sensitivity for samples in which MAT activity was low or difficult to detect, we performed a two-step reaction in which we first incubated the sample and the MAT substrates at 37°C for 20 min. We then added the HRP antibody and incubated the plate at 37°C for approximately 40 min (data not shown). If the MAT activity was not low, the MAT enzymatic reaction and competitive ELISA could be performed simultaneously. The MAT activity assay described here is a highly sensitive real-time immunoassay. Upon production of SAM, the concentration of SAM can be accurately and specifically quantified. This real-time immunoassay has several advantages: (a) the assay is highly sensitive and can accurately reflect the dynamic aspects of MAT activity; (b) this one-step, real-time method for promptly and accurately measuring synthesized SAM, an extremely unstable molecule, is superior to any other methods; and (c) this method is the fastest. This novel, accurate, convenient, and rapid method allows any laboratory to measure MAT activity easily and quickly without special equipment while providing more accurate and reliable results than Pi measurement [8], HPLC, or LC-MS/MS [9,10].

Regulation of MAT activity by Met and GSNO

Met is believed to regulate the enzymatic activity of MAT, which is critical to the regulation of SAM levels and plays crucial roles in the Met cycle and epigenetics. Therefore, we used specific antibodies against SAM and SAH to observe how cells react to Met and whether the changes in MI were results of the stimulation using LSCM after 24 h of Met stimulation in L02 and HepG2 cells for 24 h (Fig. 1). We observed SAM and SAH appear in the cytoplasm along mitochondria. In HepG2 cells, more SAM and SAH occurrence was observed surrounding the nuclei and nucleoli than in the cytoplasm. Compared with controls, there was more SAM surrounding the nuclei and nucleoli in the L02 cells after stimulation with 0.5 mM Met for 24 h, whereas there was less SAM and SAH in Met-stimulated HepG2 cells. These results indicated that Met stimulation enhances the activity of MAT-I/III but inhibits the activity of MAT-II.

To evaluate the effects of Met on MAT-II, HepG2 cells were cultured in Met-deficient MEM for 20 h, and the SAM and SAH levels were assessed by immunofluorescence LSCM using specific antibodies. The SAM levels were increased in the cytoplasm, nuclei and, in particular, the nucleoli of HepG2 cells that were Met-deprived for approximately 20 h. The SAH levels also increased after Met deprivation for 20 h. Met deficiency appears to enhance MAT-II activity in liver cell lines during the time frame observed.

The ELISA test was used to examine MAT activity under different conditions. Figure 2 shows the changes in MAT activity when L02 and HepG2 cells were stimulated with Met and GSNO. After stimulation with 0.5 mM Met for 24 h, SAM synthesis in L02 cells increased significantly. However, compared with stimulation with 0.5 mM Met, stimulation with 2 mM Met resulted in lower MAT-I/III activity. The reason for this discrepancy is unclear. In L02 cells, 1 mM GSNO significantly inhibited MAT-I/III activity regardless of the concentration of Met used, although the inhibitory effect of 1 mM GSNO on L02 cells increased as the Met concentration increased. Met inhibited MAT-II activity in HepG2 cells in a dose-dependent manner, and 1 mM GSNO had inhibitory effects on MAT-II activity in HepG2 cells, although the effect was not as strong as in L02 cells.

To further quantify the changes in SAM and SAH levels in the cytoplasm and nucleus, SAM and SAH were double-stained with different fluorescent materials in cells that were cultured and treated as indicated in Fig. 3 and analyzed using a BD FACSCanto II Flow Cytometer. The FCM results were consistent with the results of ELISA (Fig. 2) and LSCM (Fig. 1), but FCM provided more information about the changes in SAM levels in the nuclear and cytoplasmic compartments. Our results indicated that cell lines and primary cells reacted differently to Met stimulation and Met deprivation, which was likely due to differences in the initial levels of SAM and SAH. ANOVA was used to compare the geometric means of SAM and SAH. The results from the cell lines indicated that both 0.5 and 1 mM Met significantly stimulated cytoplasmic SAM production in L02 cells and significantly inhibited cytoplasmic and nuclear level of SAM in HepG2 cells. The nuclear levels of SAM in L02 cells were not significantly altered after stimulation with 0.5 mM Met but were significantly inhibited by stimulation with 1 mM Met. The changes in the SAH levels were consistent with or parallel to those of SAM in both cell lines and in both the cytoplasmic and nuclear compartments (Fig. 3A–D).

The results for primary mouse liver cells indicated that the stimulation of SAM synthesis or MAT activity

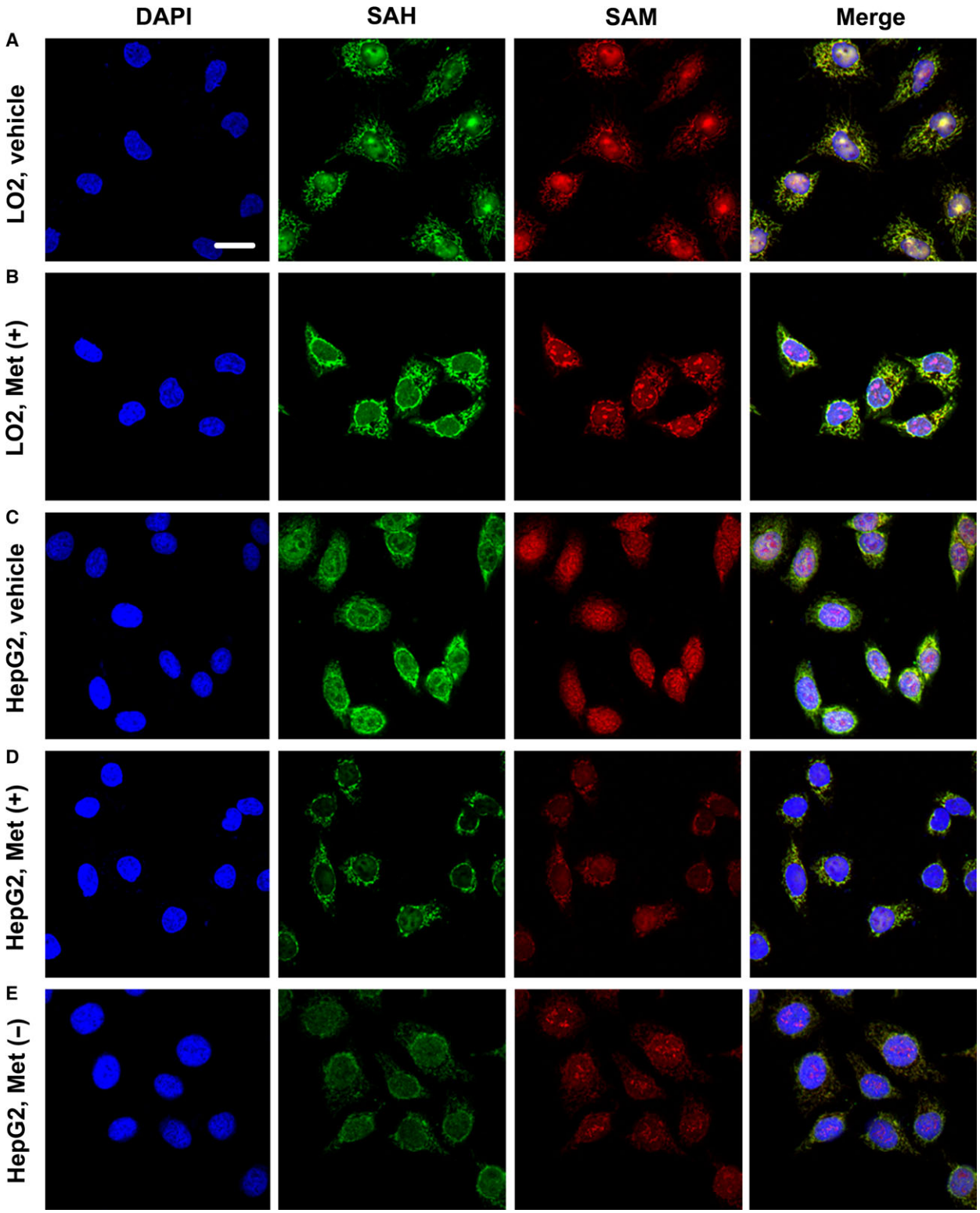

Fig. 1. Regulation of MAT activity by Met in L02 and HepG2 cells. (A, C) L02-C and HepG2-C cells with no Met added. (B, D) L02-M and HepG2-M cells with 0.5 mM Met added. (E) HepG2 cells cultured in Met-deprived MEM. The cells were observed by LSCM and photographed (×630) after 40–48 h of culture.

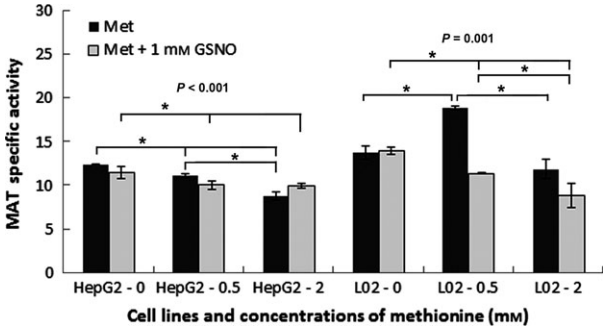

Fig. 2. Regulation of MAT activity by Met and GSNO in L02 and HepG2 cells, as determined by ELISA using cell homogenates. The concentrations of Met and GSNO used are as indicated. The number of cells from each group was normalized to 2×10^7. MAT-specific activity was defined as the amount of SAM synthesized in nM per minute per 2×10^7 cells, as described. The results are the averages of three separate experiments. The ANOVA results are shown.

by Met occurs in a dose-dependent manner only in nuclei and that Met deprivation also led to an increase in nuclear SAM synthesis (Fig. 3F). In the cytoplasm, 1 mM Met and Met deprivation inhibited MAT activity and SAM synthesis (Fig. 3E). Cytoplasmic SAH levels fluctuated with SAM under different conditions (Fig. 3G). Upon stimulation with 0.5 mM Met, nuclear methylation in primary liver cells was reduced, as nuclear SAH levels were relatively reduced but SAM levels were increased. Stimulation with a higher concentration of Met (1 mM) elevated both SAM and SAH levels. High levels of SAM were observed upon Met deprivation, whereas SAH levels in nuclei did not change upon Met deprivation (Fig. 3H).

The effects of Met-stimulated MAT activity on L02 and HepG2 cells (Fig. 3A,B, similar patterns in the cytoplasm and nucleus in both cell lines) differed from the effects on primary liver cells. In normal murine primary liver cells, approximately 4.6% of SAM was located in the nucleus, whereas in both L02 and HepG2 cells, nuclear SAM constituted 80–85% of total SAM. These results suggest that SAM may contribute significantly to cell proliferation and the immortalization of cell lines.

After stimulation with 1 mM Met for 24 h, nuclear SAM levels increased fourfold and constituted approximately 22.5% of the total SAM in primary liver cells. Met-stimulated MAT led to an increase in nuclear SAM, whereas the cytoplasmic levels of SAM decreased after 1 mM Met stimulation, indicating the possibility of migration of SAM from cytoplasm to nucleus with increased Met stimulation. When primary liver cells were cultured in Met-free medium for 20 h, MAT activity and SAM levels increased in the nucleus but decreased in the cytoplasm. These results indicated that the critical roles that SAM played in response to Met hunger/deficiency may occur in the nucleus *via* regulating the expression of certain genes accompanied by active SAM transportation across nuclear membrane.

Under the current test conditions, the MIs of L02 and HepG2 cells remained constant with and without Met stimulation, which might contribute, or be required, to maintain homeostasis in the cells. The average cytoplasmic MI of L02 was between 0.95 and 1.04, and the nuclear MI of L02 was between 1.38 and 1.48. The average cytoplasmic MI of HepG2 was between 1.31 and 1.55, and the nuclear MI of HepG2 was between 1.31 and 1.53. For primary liver cells, the average cytoplasmic MI was between 2.43 and 2.85, and the total cell MI was between 1.85 and 2.26. However, the nuclear MI was 0.31 under normal resting conditions without any stimulation and increased to 0.82 after stimulation with 0.5 mM Met and to 1.22 after stimulation with 1 mM Met. The nuclear MI was 0.98 in Met-free medium after 20 h in culture, which was approximately threefold higher than in normal resting liver cells. The changes in the MI were consistent with the changes in SAM levels.

The results above indicated that SAM and SAH levels fluctuated based on the length of time the cells were cultured and varied between the cytoplasm and nucleus. Therefore, we were interested in examining the levels of SAM and SAH at different stages of the cell proliferation cycle.

SAM and SAH levels at different stages of the cell cycle

To understand the relevance of the levels of SAM and SAH in the context of cell cycle phases, we first analyzed the percentages of different cell cycle phases in different cell lines cultured for 24 and 48 h. K562 cells and MCF cells were also compared.

As shown in Table 1, L02, K562, and MCF cells were mainly in the G0/G1 and S stages after being cultured for 24 (fast growing) and 48 h (over-growth), with some variations in the percentages of cells in the G0/G1 and/or S phases. In contrast, HepG2 cells were more frequently in the G2/M and/or S phases, and the percentage of G0/G1 cells increased significantly from 24 to 48 h. The results indicated more active DNA synthesis in HepG2 cells (45.93%) than in L02 cells (38.44%), which correlated with the higher SAM levels at 24 h in the nuclei of HepG2 cells than in L02 cells (Fig. 1C). When cell growth was faster at the 24-h

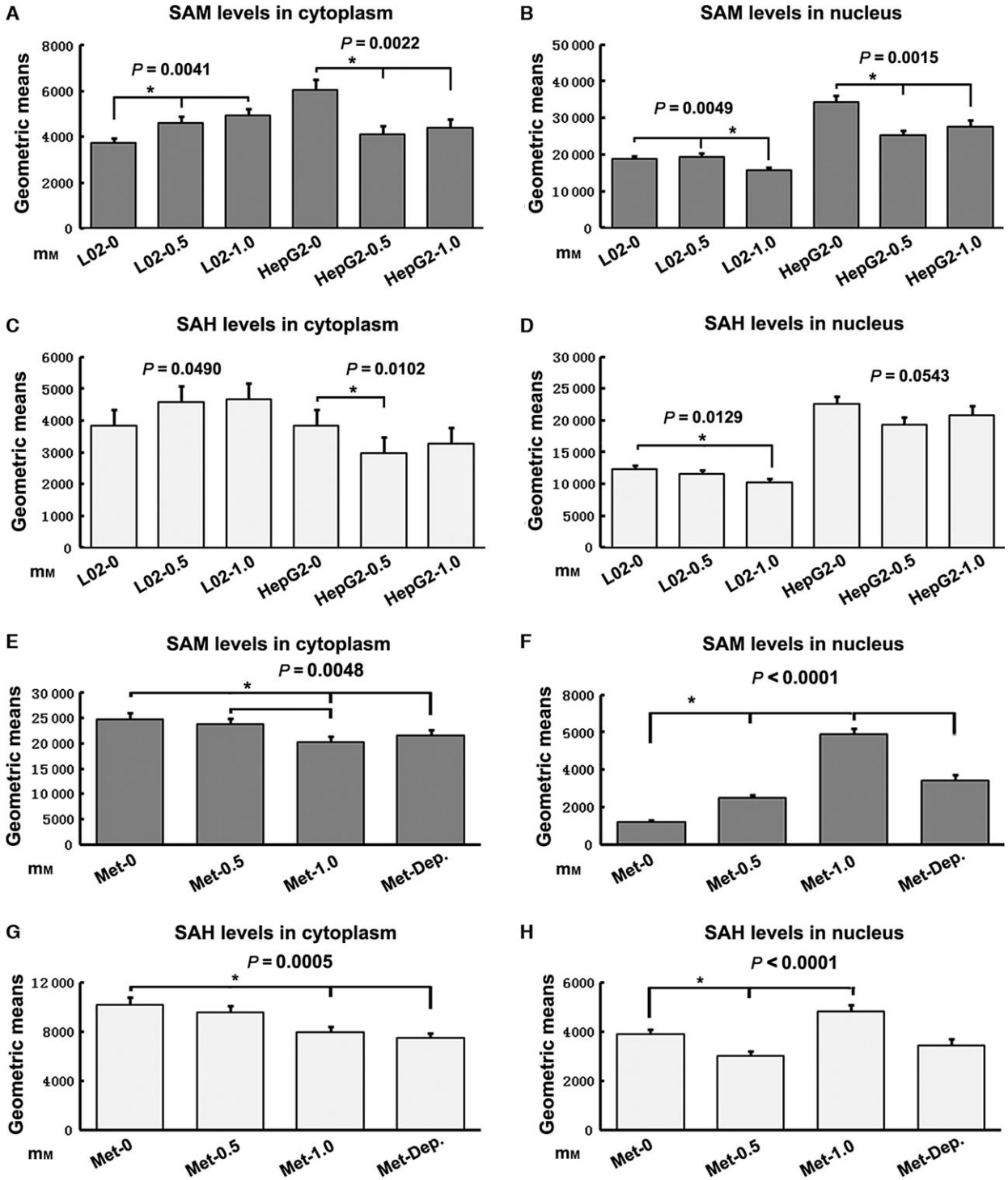

Fig. 3. Relative levels of SAM and SAH detected by FCM in the cytoplasm and nucleus of L02 and HepG2 cells compared with those in mouse primary liver cells in response to Met stimulation or deprivation (Met-Dep). (A–H): The cell types, treatment conditions, antibodies, and target details are as indicated; E–H with mouse primary liver cells. The Alexa Fluor® 647 anti-SAM antibody was used at a concentration of 4.5 $\mu g \cdot mL^{-1}$, and the Alexa Fluor® 488 anti-SAH antibody was used at a concentration of 45 $\mu g \cdot mL^{-1}$. The ANOVA results are shown.

Table 1. Percentages of cell cycle phases in cell lines cultured for different lengths of time.

Cells	G0/G1 (G1 mean)	S (%)	G2/M (G2 mean)
L02 24 h	36.19% (202)	38.44	15.67% (404)
L02 48 h	37.63% (200)	36.38	16.60% (400)
HepG2 24 h	18.96% (177)	45.93	32.35% (358)
HepG2 48 h	30.81% (195)	39.97	21.56% (390)
K562 24 h	43.85% (209)	49.62	6.73% (418)
K562 48 h	12.17% (202)	50.41	6.26% (404)
MCF 24 h	56.92% (206)	37.06	5.93% (414)
MCF 48 h	55.18% (209)	34.91	5.18% (418)

Table 2. Changes in the percentages (%) of cycle stages and means from 24 h to 48 h.

Cells	G0	S	G2	G1 mean	G2 mean
L02	3.98	−5.63	6.32	−0.99	−0.99
HepG2	62.67	−12.98	−33.35	9.23	8.94
K562	−72.25	1.59	−6.98	3.35	3.35
MCF	−3.06	−5.8	−12.65	1.45	0.97

time point, the SAM levels in the nuclei were higher in HepG2 cells than in L02 cells. When cell proliferation slowed down in the culture at the 40- and 48-h time points, the SAM levels in the nuclei were similar between unstimulated HepG2 and L02 cells, as evident in the qualitative data shown in Fig. 1A and 1C and the quantitative data shown in Fig. 2 (HepG2-0 and L02-0). These data suggested that nuclear SAM is related to DNA synthesis and probably transcriptional regulation.

Table 2 shows the changes in the percentages of cell cycle stages and the geometric means after 24 and 48 h of cell culture based on the results shown in Table 1. The proliferation properties of HepG2 cells differed from those of their normal counterparts (L02 cells) and the other malignant cell lines. These results might suggest that SAM-related or methylation-related signaling pathways were involved in cell cycle regulation and tumor transformation.

Next, SAH and SAM levels were measured using FCM at the same time points as in the cell cycle experiment in Table 1. Both SAM and SAH levels were slightly lower after 48 h than after 24 h of culture (Table 3), which was probably due to overgrowth of the cells after 48 h in culture and indicated that some cells did not proliferate or started to undergo apoptosis. These results suggested that SAM might be involved in cell proliferation and apoptosis.

Discussion

In cultured rat hepatocytes, MAT1α expression progressively decreases and MAT2α expression is induced. This switch of gene expression can be prevented by adding SAM. In cultured hepatocytes with decreased MAT1α expression, the addition of SAM increases MAT1α transcription in a dose-dependent fashion. These findings identified SAM as a key molecule that differentially regulates MAT1α and MAT2α expression and helps maintain the differentiated status of hepatocytes. *MAT1α* mRNA and protein expression have been abolished in homozygous knockout mice, and at 3 months, plasma Met levels were increased by 776% in the knockouts. Hepatic SAM and glutathione levels were reduced by 74% and 40%, respectively, whereas SAH, MTA, and global DNA methylation were unchanged. The expression of many inflammatory markers, including orosomucoid, amyloid, metallothionein, and Fas antigen, as well as growth-related genes, such as early growth response 1 and proliferating cell nuclear antigen, were increased in the knockout animals. The knockout mice were also more susceptible to choline-deficient, diet-induced fatty liver and developed spontaneous macrovesicular steatosis and predominantly periportal mononuclear cell infiltration [11]. These results indicate that SAM has anti-inflammatory and antiproliferative properties in hepatocytes. SAM can differentially regulate *MAT1α* and *MAT2α* expression and helps maintain the differentiated status of hepatocytes [12].

Table 3. Average geometric means of the FCM results in different cell lines after 24 and 48 h of culture. CP, cytoplasmic fixation/permeabilization in which only cytoplasmic targets were stained; NU, nuclear fixation/permeabilization in which both cytoplasmic and nuclear targets were stained.

Group		HepG2		L02		K562		MCF	
Antibody	Concentration ($\mu g \cdot mL^{-1}$)	CP	NU	CP	NU	CP	NU	CP	NU
AF488-anti-SAH 24 h	70	174	387	175	428	177	471	140	606
AF488-anti-SAH 48 h	70	79	365	81	312	109	349	80	275
AF647-anti-SAM 24 h	9	1587	3136	705	2565	965	2818	851	2903
AF647-anti-SAM 48 h	9	516	2295	253	1708	626	2367	477	1511

To further understand how Met differentially regulates the activity of MAT, the L02 and HepG2 cell lines were used in the present study because these cell lines express different types of MAT. We employed novel immunoassays to specifically and sensitively measure SAM levels and MAT activity after incubating the cells with Met and GSNO. Our results link damage induced by free radicals to the Met cycle and particularly to the levels of SAM. As reported previously, reduced levels of SAM are related to inflammation, and supplementation of SAM induces anti-inflammatory effects [13]. Elevated SAM levels promote the aminopropylation pathway and the production of the strongly anti-inflammatory substance MTA and the DNA-stabilizing, cell survival-related factors spermidine and spermine. However, the possibility of defective methylation leading to the accumulation of SAM should not be excluded and requires further study.

S-nitrosoglutathione is an endogenous *S*-nitrosothiol (SNO) that plays a critical role in nitric oxide (NO) signaling and is a source of bioavailable NO. NO coexists in cells with SNOs that serve as endogenous NO carriers and donors. SNOs spontaneously release NO at different rates and can be powerful terminators of free radical chain propagation reactions. Both exogenous NO and endogenous NO can react with glutathione to form GSNO. The inactivation of MAT-I/III activity through the incorporation of NO into cysteine 121 of MAT [14–16] may be one of the critical signals initiated in response to NO-induced cellular injury and impacts the synthesis of SAM. Insufficient levels of SAM have detrimental effects on the liver. In response to liver injury, the liver compensates for the damage by regenerating. In general, liver damage leads to an increase in free radicals, which, in turn, inhibits MAT-I/III activity. The inhibition of MAT activity prevents the normal consumption and use of the energy molecule ATP, which endangers the survival of liver cells. Liver function, regeneration, differentiation, and sensitivity to injury are also impacted by reduced or defective SAM synthesis [2]. SAM-depleted animals exhibit tissue injury, necrosis and inflammatory infiltration. Given the critical roles of SAM and MAT in liver proliferation, differentiation, and apoptosis, the epigenetic regulation of MAT could be targeted for the development of treatments for hepatocellular carcinoma (HCC) [17].

The current work using accurate, sensitive, and specific assays to measure MAT activity and SAM levels showed that 0.5 mM Met stimulated MAT-I/III activity, GSNO inhibited MAT-I/III activity, and the MI increased in L02 cells after Met stimulation. In contrast, in HepG2 cells, MAT-II activity was inhibited by 0.5 mM Met and slightly by 1 mM GSNO and the MI decreased after Met stimulation. HepG2 cells exhibited deficient methylation, and Met stimulation initiated DNA methyltransferase activity, causing a reduction in SAM levels and an increase in SAH in the nuclei. Using the specific anti-SAM and anti-SAH antibodies and the immunoassays, we were able to quickly, easily, sensitively, and accurately quantify SAM, SAH and MAT activity and determine their cellular localizations. The MI was also evaluated quickly and accurately to reflect the methylation capability and status of cells. The novel methods used here will help address important questions related to methylation and the Met cycle.

The results reported in Tables 1–3 suggested that SAM and/or SAM/SAH play important roles in the malignant transformation, proliferation, and apoptosis of liver cells; these findings are consistent with other reports [9,18–23]. Therefore, SAM level could be a critical switch in the regulation of hepatocyte proliferation, regeneration, and response to injury [24–28].

Mammalian embryonic development is a tightly regulated process that produces a large number of cell types with highly divergent functions from a single zygote. Distinct cellular differentiation programs are facilitated by tight transcriptional and epigenetic regulation. Epigenetic regulation is thought to contribute to tissue homeostasis after the completion of development. Depending on the tissue type and the epigenetic regulators affected, the consequences of epigenetic alterations may include the disruption of tissue homeostasis, which may predispose the organism to diseases such as cancer [29]. Researchers have become increasingly aware of the role of epigenetic factors in the risk of cancer. The MI reflects the methylation capability and methylation status of cells. Changes in methylation are closely related to normal cell functions, the individual development of carcinogenesis, and stem cell reprogramming; these changes may have implications for the development of novel diagnostic tools and therapies [30].

Imprinting is defined as the parental allele-specific expression of genes with lengths of 50–80 bp. The regulation of imprinting depends on the epigenetic marking of the parental alleles during gametogenesis. Monoallelic expression ensures that the imprinted genes encode the correct levels of proteins, including important factors involved in embryonic growth, placental growth, and adult metabolism. The regulation of imprinted genes is largely dependent on methylation marks that are read by imprinting control regions

(ICRs) using one of two mechanisms, chromatin barrier formation or untranslated RNAs, to ensure that only the maternal or paternal allele is expressed [31]. It is increasingly clear that although epigenetic factors do not affect the primary sequence of the genome, they play important roles in cell growth and carcinogenesis. Genomes undergo changes in their methylation state, and the control of parental allele-specific methylation and the expression of imprinted loci is lost (LOI) in many cancers. Many of the loci that exhibit aberrant methylation in cancer have since been identified and have been shown to be silenced by DNA methylation. In contrast to gene mutations that are basically irreversible, methylation modifications are reversible, which raises the possibility of developing therapeutics based on restoring the normal methylation state of cancer-associated genes [32]. The important transcription factor CCCTC-binding factor (CTCF) has been shown to mediate the functions of ICR. CTCF is an ubiquitously expressed and exceptionally highly conserved multifunctional protein that binds *via* its 11-zinc finger DNA-binding domain to target sites with remarkable sequence variation [33,34]. The binding of CTCF to several sites in the unmethylated ICR [35–37] is essential for blocking the function of enhancers and forming the insulator complex.

Methionine adenosyltransferase activity determines the levels of SAM and the MI and thus affects the methylation status of DNA. Our results indicate that there are correlations among changes in MAT activity, SAM levels, methylation status, the cell cycle, and HCC. A recent study [36] of HCC DNA methylation reported that the methylation status of a large panel of imprinted genes is deregulated in HCC, suggesting a major role in hepatocarcinogenesis. *In vitro* models support the hypothesis that imprinted gene methylation is a potential marker for environmental exposure to risk factors such as infection with hepatitis virus and lipid accumulation in the liver.

Conclusions

In this study, immunoassays to accurately, sensitively, and specifically measure MAT activity and SAM and SAH levels in cells and cell homogenates have been established. These methods have many advantages over previous methods used to measure MAT activity and the MI. In L02 cells, MAT-I/III activity was stimulated by 0.5 mM Met, GSNO inhibited MAT-I/III activity, and the MI increased after Met stimulation. In HepG2 cells, Met and GSNO inhibited MAT-II activity, and the MI decreased after Met stimulation. The cellular localization of SAM and SAH in the nuclei, nucleoli, and mitochondria was described for the first time in this report. The levels and localization of both SAM and SAH responded sensitively and quickly to the proliferation, growth, and apoptosis status of cells, and the regulation of MAT activity and the value of MI correlated well with the occurrence of HCC.

Author contributions

XH designed and performed some of the experiments, contributed to the writing, editing, and proofreading of the manuscript. MZ performed the experiments, analyzed the data, and contributed to the writing and editing of the manuscript. HL performed some of the experiments. IAA proofread the manuscript.

References

1 Finkelstein JD (1990) Methionine metabolism in mammals. *J Nutr Biochem* **1**, 228–236.
2 Corrales FJ, Pérez-Mato I, Sánchez Del Pino MM, Ruiz F, Castro C, García-Trevijano ER, Latasa U, Martínez-Chantar ML, Martínez-Cruz A, Avila MA *et al.* (2002) Regulation of mammalian liver methionine adenosyltransferase. *J Nutr* **132** (8 suppl), 2377s–2381s.
3 Mato JM, Alvarez L, Ortiz P and Pajares MA (1997) S-Adenosylmethionine synthesis: molecular mechanisms and clinical implications. *Pharmacol Ther* **73**, 265–280.
4 Gil B, Casado M, Pajares MA, Boscá L, Mato JM, Maetin-Sanz P and Alvarez L (1996) Differential expression pattern of S-adenosylmethionine synthetase isoenzymes during rat liver development. *Hepatology* **24**, 876–881.
5 Sánchez del Pino MM, Corrales FJ and Mato JM (2000) Hysteretic behavior of methionine adenosyltransferase III. *J Biol Chem* **275**, 23476–23482.
6 Ilisso CP, Sapio L, Delle Cave D, Illiano M, Spina A, Cacciapuoti G, Naviglio S and Porcelli M (2016) S-Adenosylmethionine affects ERK1/2 and Stat3 pathways and induces apoptosis in osteosarcoma cells. *J Cell Physiol* **231**, 428–435.
7 Lu SC (2000) S-Adenosylmethionine. *Int J Biochem Cell Biol* **32**, 391–395.
8 Fernández-Irigoyen J, Santamaría E, Chien YH, Hwu W, Korman SH, Faghfoury H, Schulze A, Hoganson GE, Stabler SP, Allen RH *et al.* (2010) Enzymatic activity of methionine adenosyltransferase variants identified in patients with persistent hypermethioninemia. *Mol Genet Metab* **101**, 172–177.
9 Avila MA, Carretero MV, Rodriguez EN and Mato JM (1998) Regulation by hypoxia of methionine adenosyltransferase activity and gene expression in rat hepatocytes. *Gastroenterology* **114**, 364–371.

10 Martínez-Chantar ML, Latasa MU, Varela-Rey M, Lu SC, García-Trevijano ER, Mato JM and Avila MA (2003) L-methionine availability regulates expression of the methionine adenosyltransferase 2A gene in human hepatocarcinoma cells role of S-adenosylmethionine. *J Biochem* **278**, 19885–19890.
11 Lu SC, Alvarez L, Huang ZZ, Chen L, An W, Corrales FJ, Avila MA, Kanel G and Mato JM (2001) Methionine adenosyltransferase 1A knockout mice are predisposed to liver injury and exhibit increased expression of genes involved in proliferation. *Proc Natl Acad Sci USA* **98**, 5560–5565.
12 García-Trevijano ER, Latasa MU, Carretero MV, Berasain C, Mato JM and Avila MA (2000) S-Adenosylmethionine regulates MAT1A and MAT2A gene expression in cultured rat hepatocytes: a new role for S-adenosylmethionine in the maintenance of the differentiated status of the liver. *FASEB J* **14**, 2511–2518.
13 Najm WI, Reinsch S, Hoehler F, Tobis JS and Harvey PW (2004) S-Adenosyl methionine (SAMe) versus celecoxib for the treatment of osteoarthritis symptoms: a double-blind cross-over trial. *BMC Musculoskelet Disord* **5**, 6–20.
14 Avila MA, Mingorance J, Martínez-Chantar ML, Casado M, Martin-Sanz P, Bosca L and Mato JM (1997) Regulation of rat liver S-adenosylmethionine synthetase during septic shock: role of nitric oxide. *Hepatology* **25**, 391–396.
15 Pérez-Mato I, Castro C, Ruiz FA, Corrales FJ and Mato JM (1999) Methionine adenosyltransferase S-nitrosylation is regulated by the basic and acidic amino acids surrounding the target thiol. *J Biol Chem* **274**, 17075–17080.
16 Ruiz F, Corrales FJ, Miqueo C and Mato JM (1998) Nitric oxide inactivates rat hepatic methionine adenosyltransferase In vivo by S-nitrosylation. *Hepatology* **28**, 1051–1057.
17 Yang H, Cho ME, Li TW, Peng H and Ko KS (2013) Epigenetic regulation of methionine adenosyltransferase 1A: a role for microRNA-based treatment in liver cancer? *Hepatology* **57**, 2081–2084.
18 Frau M, Tomasi ML, Simile MM, Demartis MI, Salis F, Latte G, Calvisi DF, Seddaiu MA, Daino L, Feo CF *et al.* (2012) Role of transcriptional and posttranscriptional regulation of methionine adenosyltransferases in liver cancer progression. *Hepatology* **56**, 165–175.
19 Lu SC and Mato JM (2005) Role of methionine adenosyltransferase and S-adenosylmethionine in alcohol-associated liver cancer. *Alcohol* **35**, 227–234.
20 Pañeda C, Gorospe I, Herrera B, Nakamura T, Fabregat I and Varela-Nieto I (2002) Liver cell proliferation requires methionine adenosyltransferase 2A mRNA up-regulation. *Hepatology* **35**, 1381–1391.
21 Stiuso P, Bagarolo ML, Ilisso CP, Vanacore D, Martino E, Caraglia M, Porcelli M and Cacciapuoti G (2016) Protective effect of tyrosol and S-adenosylmethionine against ethanol-induced oxidative stress of Hepg2 cells involves Sirtuin 1, P53 and Erk1/2 signaling. *Int J Mol Sci* **17**, 622.
22 Li TW, Yang H, Peng H, Xia M, Mato JM and Lu SC (2012) Effects of S-adenosylmethionine and methylthioadenosine on inflammation-induced colon cancer in mice. *Carcinogenesis* **33**, 427–435.
23 Yang H, Magilnick N, Noureddin M, Mato JM and Lu SC (2007) Effect of hepatocyte growth factor on methionine adenosyltransferase genes and growth is cell density-dependent in HepG2 cells. *J Cell Physiol* **210**, 766–773.
24 Kharbanda KK (2009) Alcoholic liver disease and methionine metabolism. *Semin Liver Dis* **29**, 155–165.
25 Kiani S, Ebrahimkhani MR, Shariftabrizi A, Doratotaj B, Payabvash S, Riazi K, Dehghani M, Honar H, Karoon A, Amanlou M *et al.* (2007) Opioid system blockade decreases collagenase activity and improves liver injury in a rat model of cholestasis. *J Gastroenterol Hepatol* **22**, 406–413.
26 Lu SC and Mato JM (2012) S-adenosylmethionine in liver health, injury, and cancer. *Physiol Rev* **92**, 1515–1542.
27 Lu SC, Tsukamoto H and Mato JM (2002) Role of abnormal methionine metabolism in alcoholic liver injury. *Alcohol* **27**, 155–162.
28 Zhang L, Liu XH, Qi HB, Li Z, Fu XD, Chen L and Shao Y (2015) Ursodeoxycholic acid and S-adenosylmethionine in the treatment of intrahepatic cholestasis of pregnancy: a multi-centered randomized controlled trial. *Eur Rev Med Pharmacol Sci* **19**, 3770–3776.
29 Avgustinova A and Benitah SA (2016) Epigenetic control of adult stem cell function. *Nat Rev Mol Cell Biol* **76**, 1–13.
30 Kaneda A and Feinberg AP (2005) Loss of imprinting of IGF2: a common epigenetic modifier of intestinal tumor risk. *Cancer Res* **65**, 11236–11240.
31 Jelinic P and Shaw P (2007) Loss of imprinting and cancer. *J Pathol* **211**, 261–268.
32 Plass C and Soloway PD (2002) DNA methylation, imprinting and cancer. *Eur J Hum Genet* **10**, 6–16.
33 Mukhopadhyay R, Yu W, Whitehead J, Xu J, Lezcano M, Pack S, Kanduri C, Kanduri M, Ginjala V, Vostrov A *et al.* (2004) The binding sites for the chromatin insulator protein CTCF map to DNA methylation-free domains genome-wide. *Genome Res* **14**, 1594–1602.
34 Ong CT and Corces VG (2014) CTCF: an architectural protein bridging genome topology and function. *Nat Rev Mol Cell Biol* **15**, 234–246.

35 Bell AC and Felsenfeld G (2000) Methylation of a CTCF-dependent boundary controls imprinted expression of the Igf2 gene. *Nature* **405**, 482–485.
36 Lambert MP (2015) Aberrant DNA methylation of imprinted loci in hepatocellular carcinoma and after in vitro exposure to common risk factors. *Clin Epigenetics* **7**, 15.
37 Ohlsson R, Renkawitz R and Lobanenkov V (2001) CTCF is a uniquely versatile transcription regulator linked to epigenetics and disease. *Trends Genet* **17**, 520–527.